BeBeC-2022-S04

Berlin Beamforming Conference

VIRTUAL MICROPHONE ARRAY ROTATION IN THE MODE-TIME DOMAIN AND SEPARATION OF STATIONARY AND ROTATING SOUND SOURCES IN AN AXIAL FAN

Gert Herold, Simon Jekosch, Tobias Jüterbock, Ennes Sarradj
Technische Universität Berlin, Department of Engineering Acoustics
Einsteinufer 25, 10587 Berlin, Germany

Abstract

Acoustic measurement data of axial fans contains rotating as well as stationary noise sources. While it is possible to use microphone array methods to focus on both kinds of sources, some contamination of the respective other source type is always present in the evaluations. This paper explores the capabilities of array methods working in the mode domain to separate rotating and non-rotating noise, visualize the respective source distributions and determine detailed spectral characteristics of selected components.

1 Introduction

Efficient measures to influence the acoustic emission of fans necessitate knowledge about noise generating mechanisms. Microphone array methods such as acoustic beamforming have proven to be a valuable tool for the identification and characterisation of sound sources radiating from different components. The idea behind such methods is to spatially filter the sound imission by shifting the received signals such that only sound emitted from a currently focused location is passed unattenuated [1]. By scanning multiple focus points within a region of interest, a sound map can be generated.

In axial fans, important sources can be expected to rotate synchronously with the blades, which makes it necessary to compensate the rotating motion during the array data processing. This can be done in the time domain by continuously adjusting the signal time shift according to a rotating focus point [6, 10]. Alternatively, by using suitable array geometries, a virtual array rotating synchronously with the fan can be synthesized based on time data measured by stationary sensors [4, 8]. The latter processing has the advantage that with the transformation of the data into the rotating reference frame, microphone array methods that can only be used for stationary sources (e.g. frequency domain beamforming) can now be applied on rotating sources as well.

The type of sound sources present in practical applications is often not exclusively rotating or stationary. This means that in any reference frame – rotating or stationary – there will be a number of sources that are non-stationary, i.e. rotating. The acoustic energy of those sources will be "smeared" around the axis of rotation. With a sufficiently long measurement time, the energy will distribute evenly over the circumference and thus allow dominant stationary sources to still be visible. However, this "rotation noise" can be expected lead to a decrease in the signal-to-noise ratio and may mask some weaker sources.

In this contribution, a method to decrease the contamination of data with rotation noise in the current frame of reference is presented. First, the theory of virtual rotation and beamforming is briefly revisited and formulated in the mode domain. Then, the data processing for denoising using classic frequency beamforming without the main-diagonal of the cross-spectral matrix in the mode domain (CSM-M) is explained. Finally, the methods are applied to measurement data of an axial fan with five blades, and the evaluation results are discussed.

2 Methods

2.1 Virtual rotating array

The idea behind the virtual rotating array (VRA) method is to synthesize array data in the rotating reference frame by interpolating data between sensors of a physical circular array [4]:

$$p_{\mathrm{rot}}(l_{\mathrm{rot}},t) = p(l_{\mathrm{stat}} + M \cdot \frac{\varphi(t)}{2\pi}, t) \ . \tag{1}$$

M is the number of equally distributed microphones in the ring, l describes the coordinate (i.e. the index) of the virtual rotating or stationary microphone. The current rotation angle is described by $\varphi(t)$. A linear interpolation of data between neighboring sensors has been shown to be not as reliable at higher frequencies as synthesizing the signals in the mode-frequency domain [3, 7]. For this, the data is fourier-transformed from the spatial into the mode domain and from the time into the frequency domain. Subsequently, the mode spectra are shifted according to the rotational speed [8], which, however, has to be constant for this.

If the Fourier transform is done only from the spatial into the mode domain

$$p(m,t) = \frac{1}{\sqrt{M}} \sum_{l=-M/2}^{M/2-1} p(l,t)\, \mathrm{e}^{-\mathrm{j}2\pi m \frac{l}{M}} \ , \tag{2}$$

the virtual rotation can be done simply by [2]:

$$p_{\mathrm{rot}}(m,t) = \mathrm{e}^{\mathrm{j}m\varphi(t)} \cdot p(m,t) \ . \tag{3}$$

2.2 Beamforming in the frequency domain

For approximating the incident acoustic energy from one focus point and for one frequency, the classic frequency domain beamforming formulation can be evaluated [1]:

$$|p_{\mathrm{out}}|^2 = \boldsymbol{h}^{\mathrm{H}} \boldsymbol{C} \boldsymbol{h} \,. \tag{4}$$

The steering vector $\boldsymbol{h}$ contains the transfer functions from the focus point to all sensor positions, taking into account the sound propagation through the medium and also weighting the microphone signals. $\boldsymbol{C}$ is the cross-spectral matrix (CSM), calculated according to Welch's method [11] by dividing the time signal into blocks of fixed length, transforming from time into frequency domain, calculating the cross-spectra, and averaging the resulting matrices.

In contrast to the usual processing by correlating the recorded time-data between microphone channels, the cross-spectra here are calculated between the modes, i.e. the data has to be transformed into the mode domain by a spatial Fourier transform (see Eq. (2)) before. If the steering vectors are also transformed into the mode domain, Eq. (4) yields the exact same result as in the spatial domain [2].

For array measurements in an aeroacoustic context, it is common practice to omit the main diagonal of the CSM in the calculations, as it contains additional self-noise that decreases the signal-to-noise ratio (SNR) of the result [1]. For the CSM in the spatial domain, this self-noise could for instance be caused by flow over the microphones. When calculating the CSM in the mode domain, the main diagonal (autospectra) additionally holds the contribution of sources which appear rotating in the current reference frame, whereas in the off-diagonal entries (cross-spectra), these average out with increasing number of blocks [2].

This means that by virtually rotating the data with the fan, the influence of stationary sources can be decreased by subsequent beamforming in the mode domain without the CSM main diagonal. Conversely, the SNR of stationary sources can be improved by the same technique without prior virtual rotation.

2.3 Source power integration

For the spatial separation of sources, Eq. (4) is evaluated for a set of focus positions that discretize a region of interest, generating a sound map. For a quantitative analysis, the squared sound pressures of the reconstructed sources can be summed over the whole region or parts of it.

Since, however, the classic beamforming result contains imaging artefacts in that it displays point sources with a spatial extent and side lobes (the point spread function, PSF), such an integration would overestimate the energy in the map. Therefore, the calculated maps for each frequency are normalized prior to an integration by the according PSF of a point source positioned in the center of the focus region [9].

3 Experiments

Measurements were performed in the anechoic room at the Department of Engineering Acoustics at TU Berlin. The measurement object is a 5-bladed axial fan set in a plate as shown in Fig. 1. The array consists of 64 microphones evenly distributed on a ring with a diameter of 2.09 m and is axially aligned with the rotation axis of the fan. Two cases were considered: one with

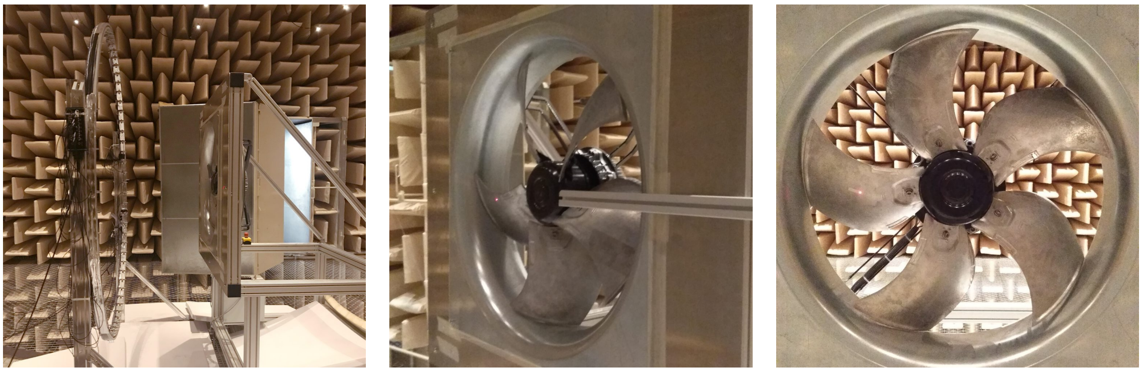

Figure 1: From left: side view of the array ring with the fan rig, fan with the interfering rod installed, view of the fan from the suction side as seen by the array.

Table 1: Measurement parameters.

microphone array	$M = 64$ axially centered ring $d_{\text{array}} = 2.09\,\text{m}$
sampling rate	$f_{\text{s}} = 51\,200\,\text{Hz}$
measurement time	40 s
tacho signal	1 trigger per revolution
environment	freefield
speed of sound	$c = 344.1\,\frac{\text{m}}{\text{s}}$
distance to focus plane	0.82 m
rotational speed	$f_{\text{rot}} = -17.5\,\text{Hz}$
rotor	5 forward-skewed blades
stator	4 struts
rod diameter	40 mm

the fan rotating in a mostly undisturbed flow, and a second where a rod obstructing the flow was installed on the suction side. The array was positioned about 80 cm upstream of the fan. Important measurement parameters are summarized in Table 1.

Beamforming is calculated in a circular region encompassing the rotor plane. The focus area is discretized by equally distributed points with about 1 cm distance. All evaluations are done in the mode domain, with the full main diagonal of the CSM as well as with omitting it in the

Table 2: Evaluation parameters.

FFT block size	4096 (narrow band 12.5 Hz)
FFT window	von Hann, 50 % overlap
focus grid	circular area equally discretized $d_{\text{focus}} = 1\,\text{m}, \Delta r \approx 0.01\,\text{m}$

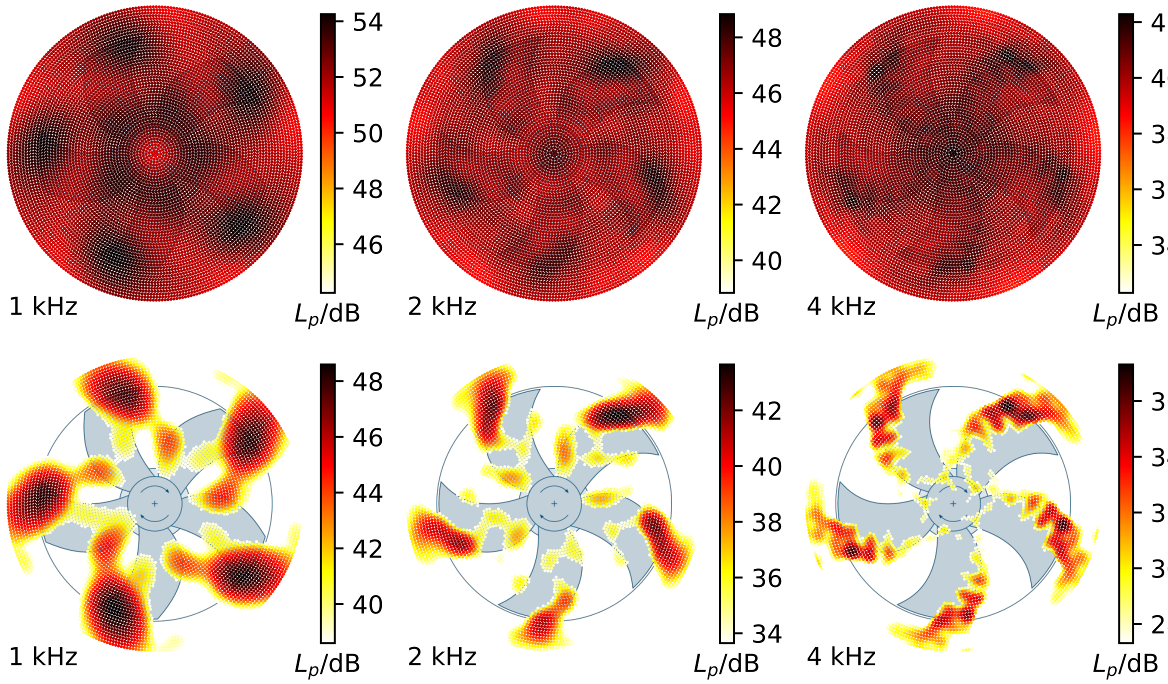

Figure 2: Sound maps with 10 dB dynamic for the case with the obstructing rod installed. Evaluated in the rotating reference frame for exemplary frequencies (1/3-octave bands). Top row: CSM with full main diagonal; bottom row: CSM main diagonal removed.

calculations. Important evaluation parameters are summarized in Table 2.

4 Results

4.1 Sound maps

Exemplary sound maps for the measurement with the flow-obstructing rod are shown in Figures 2 and 3. Evaluated are the 1/3-octave bands around 1, 2, and 4 kHz. The displayed dynamic range is 10 dB for each map, with the respective maximum represented in black. For both cases it becomes clearly visible that the removal of the main diagonal leads to a significant increase of the visible dynamic range, i.e. the SNR of the reconstructed sources.

In the rotating case (Fig. 2), the removal of rotation noise reveals several regions where noise is generated. At 1 kHz, the dominant sources are positioned at the leading edges of the blade tips. Other sources can be seen at the center section of the blade, again leading edges, and close to the hub, starting from the middle of the chord extending towards the trailing edges at higher radii.

Those secondary sources can still be seen at 2 kHz, with the first one separating into two sources: one at the very leading edge a little closer to the tip of the blades and the other closer to the base and more towards the center of the chord. The dominant sources at the tip region can be found at the trailing edges for this frequency band.

For the 4 kHz third-octave band, sources can be found mostly at the trailing edges along the whole span. There appear two separate source regions at the blade tips: one at the very tip a little

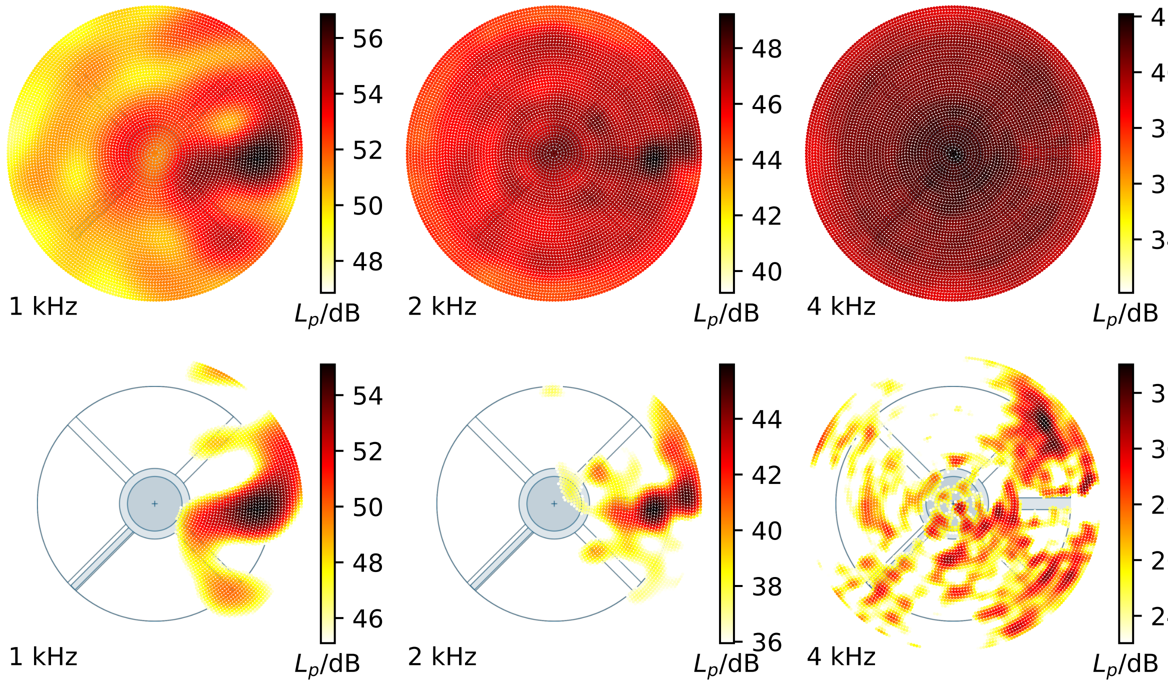

Figure 3: Sound maps for the case with the obstructing rod installed. Evaluated in the stationary reference frame for exemplary frequencies (1/3-octave bands). Top row: CSM with full main diagonal; bottom row: CSM main diagonal removed.

before the trailing edges and the other right after the trailing edges and at slightly smaller radii. Several minor sources at the hub and at the blade base leading edges can be seen as well.

The sound maps in the stationary reference frame (Fig. 3) show that at 1 kHz and 2 kHz, the rod is indeed responsible for a significant part of the noise generation. Aside from this, however, it can be seen that at the struts on the right side, there is some sound generation happening as well. At 4 kHz, the rod is not the driver of noise generation anymore. Instead, the regions near the struts at higher radii appear to become important.

4.2 Integrated spectra

For a quantitative assessment, narrow band sound maps for the case with and without rod are integrated using the source power integration method and shown in Fig. 4. For the calculations in the rotating reference frame and when omitting the CSM main diagonal, the levels are decreased by 20 dB to 25 dB at lower frequencies (about 100 Hz) compared to the calculations including the diagonal. For higher frequencies (around 1 kHz and above), the difference decreases to about 10 dB to 15 dB. While at lower frequencies, the spectra with and without the rod differ, they are mostly identical above 2 kHz with diagonal removal, showing the acoustic influence of the rod can be completely removed here.

In the stationary reference frame (Fig. 4b), the level decrease is not as significant as in the rotating frame, with 20 dB without the rod and 5 dB to 15 dB with the rod installed. This hints at the stationary sources overall being dominant, in particular with the obstructing rod present in

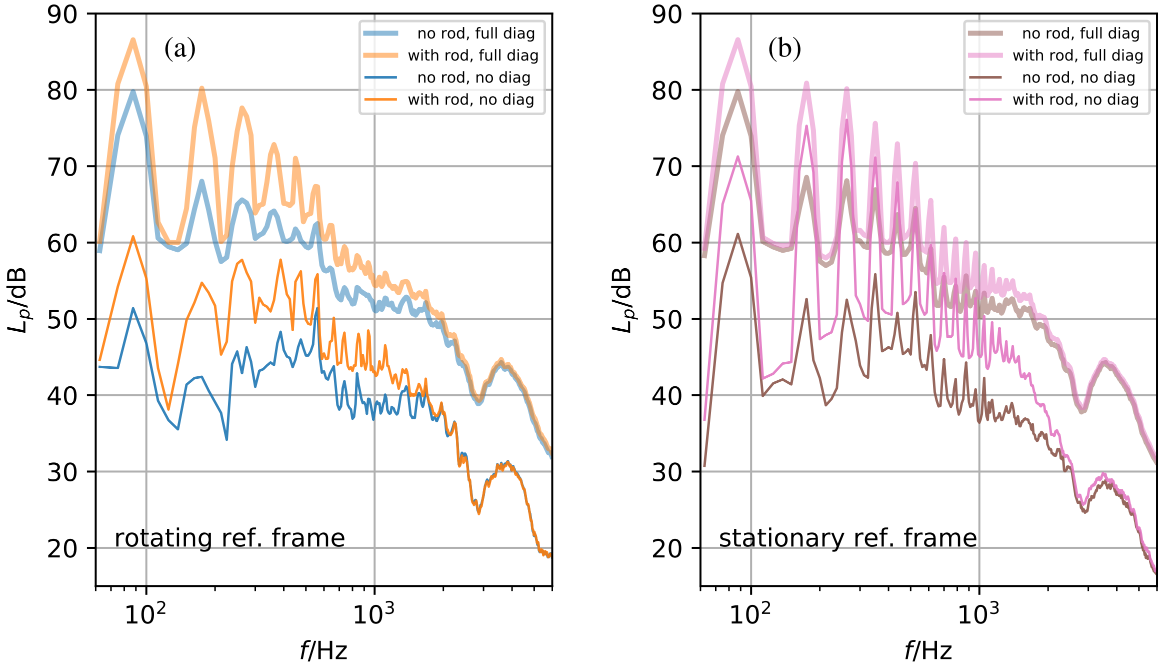

Figure 4: Spectra in the rotating and the stationary reference frame (integrated over whole focus area).

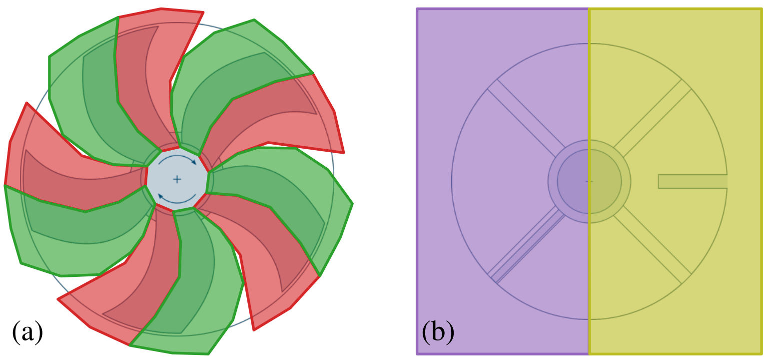

Figure 5: Integration regions used for the (a) rotating and the (b) stationary reference frame.

the flow field. At higher frequencies, the spectral curves of the two cases are closer to another as well. However, the exact levels also differ with the evaluation with removed diagonal (higher levels with the rod).

In both reference frames, tonal components present in the spectra at around 1 kHz become better visible with the removal of the rotation noise.

For a more detailed insight of the influence of the presence of the flow disturbance introduced by the rod, spectra are now integrated over sub-regions of the map: the leading and trailing edges for the rotating reference frame and the left and right sides (the latter containing the rod) of the

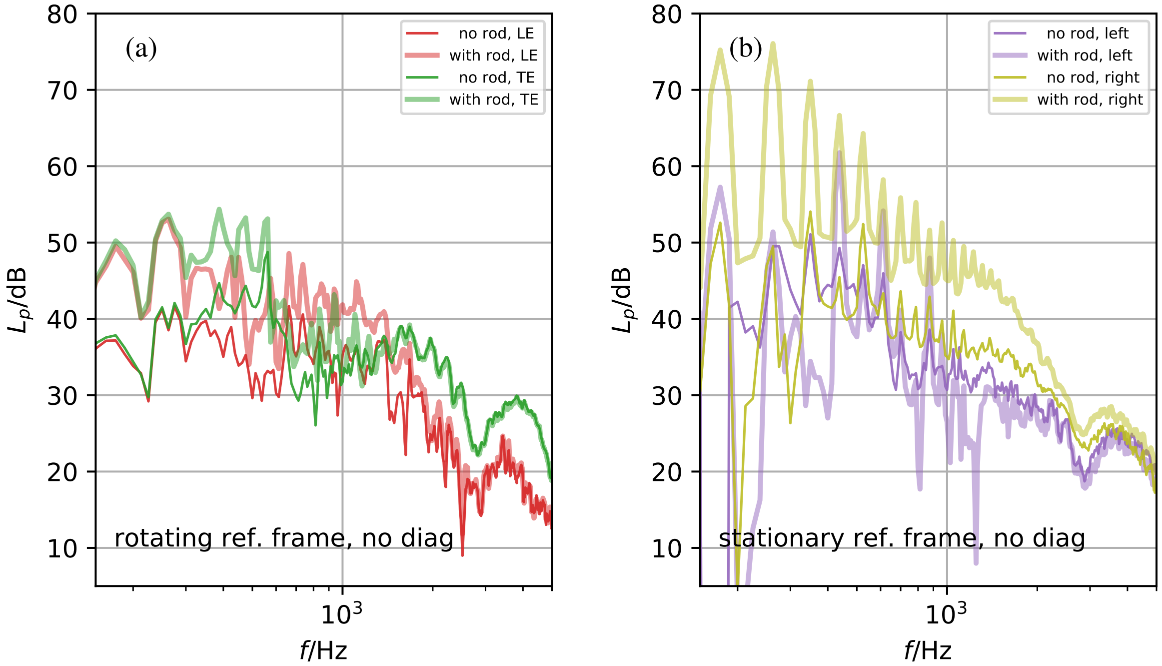

Figure 6: Rotating and stationary narrow band spectra integrated over sub-regions as defined in Fig. 5. CSM main diagonal omitted in the evaluations.

map for the stationary frame. The respective integration sectors are highlighted in Fig. 5.

As can be seen in Fig. 6a, the contribution of leading edges (LE) and trailing edges (TE) to the overall sound emission depends on the frequency. The apparent equality of the levels at and below 300 Hz hints at the resolution limit of the array being reached, so that sources can not be separated here any more.

At around 1.3 kHz and above, the TE regions contain most sound energy. For frequencies between 800 Hz and 1.3 kHz, LE noise and TE noise have more or less equal levels for the case without the rod, whereas with the rod present, LE noise is dominant. The trailing edge noise becoming dominant at higher frequencies is in line with observations found for other axial fans [5, 12, 13]. Interestingly, the noise levels from the TE regions appear to exceed the noise radiated from the LE regions for frequencies between 300 and 600 Hz. Whether this can be attributed to an actual source mechanism located at these positions or to emerging modal structures at these frequencies remains to be investigated.

Looking at the integrated spectra in the stationary domain (Fig. 6b), it becomes even clearer that the rod is responsible for most of the noise generation in this setup. Even though the right sector appears to be dominant over a wide frequency range in the case with free inflow as well, the levels are significantly higher if the inflow is disturbed by the rod. Comparing the rotating and stationary frame spectra in Fig. 6 side-by-side, it can be also seen that the nature of the dominant source introduced with the rod is stationary.

5 Conclusion

A new method for separating stationary and rotating noise components present in a data set has been applied to measurement data of an axial fan. It has been shown that the method is capable of increasing the SNR in the respective frame of reference, revealing source mechanisms that otherwise would have been masked by rotation noise. Spectra integrated over sub-regions help with a deeper understanding of the underlying noise generating mechanisms and to which aspect of the flow field they can be attributed.

References

[1] R. P. Dougherty. "Beamforming in acoustic testing." In *Aeroacoustic Measurements* (edited by T. J. Mueller), pages 62–97. Springer, Berlin, Heidelberg, 2002. doi:10.1007/978-3-662-05058-3_2.

[2] G. Herold. *One Ring to Find Them All – Detection and Separation of Rotating Acoustic Features with Circular Microphone Arrays*. Ph.D. thesis, Technische Universität Berlin, 2021. doi:10.14279/depositonce-12591.

[3] G. Herold, C. Ocker, E. Sarradj, and W. Pannert. "A comparison of microphone array methods for the characterization of rotating sound sources." In *Proceedings of the 7th Berlin Beamforming Conference*, pages 1–12. Berlin, Germany, 2018.

[4] G. Herold and E. Sarradj. "Microphone array method for the characterization of rotating sound sources in axial fans." *Noise Control Engineering Journal*, 63(6), 546–551, 2015. doi:10.3397/1/376348.

[5] G. Herold, F. Zenger, and E. Sarradj. "Influence of blade skew on axial fan component noise." *International Journal of Aeroacoustics*, 16(4-5), 418–430, 2017. doi:10.1177/1475472X17718740.

[6] O. Minck, N. Binder, O. Cherrier, L. Lamotte, and V. Budinger. "Fan noise analysis using a microphone array." In *Fan 2012 - International Conference on Fan Noise*, pages 18–20. Senlis, France, 2012.

[7] C. Ocker, G. Herold, F. Krömer, W. Pannert, E. Sarradj, and S. Becker. "A comparison of frequency-domain microphone array methods for the characterization of rotating broadband noise sources." *Acta Acustica united with Acustica*, 105(1), 66–74, 2019. doi:10.3813/aaa.919288.

[8] W. Pannert and C. Maier. "Rotating beamforming – motion-compensation in the frequency domain and application of high-resolution beamforming algorithms." *Journal of Sound and Vibration*, 333(7), 1899–1912, 2014. doi:10.1016/j.jsv.2013.11.031.

[9] P. Sijtsma. "Phased Array Beamforming Applied to Wind Tunnel and Fly-Over Tests." *SAE Technical Papers*, 2010-Octob(October), 17–19, 2010. doi:10.4271/2010-36-0514.

[10] P. Sijtsma, S. Oerlemans, and H. Holthusen. "Location of rotating sources by phased array measurements." In *Proceedings of the 7th AIAA/CEAS Aeroacoustics Conference*, pages 1–11. Maastricht, Netherlands, 2001. doi:10.2514/6.2001-2167.

[11] P. D. Welch. "The use of fast Fourier transform for the estimation of power spectra: a method based on time averaging over short, modified periodograms." *IEEE Transactions on Audio and Electroacoustics*, 15(2), 70–73, 1967. doi:10.1109/TAU.1967.1161901.

[12] S. E. Wright. "The acoustic spectrum of axial flow machines." *Journal of Sound and Vibration*, 45(2), 165–223, 1976. doi:10.1016/0022-460X(76)90596-4.

[13] F. J. Zenger, G. Herold, S. Becker, and E. Sarradj. "Sound source localization on an axial fan at different operating points." *Experiments in Fluids*, 57(8), 1–10, 2016. doi: 10.1007/s00348-016-2223-8.